

Texture and stretch formability of rolled Mg–Zn–RE (Y, Ce, and Gd) alloys at room temperature

Zheng-Xu Cai, Hai-Tao Jiang*, Di Tang,
Zhao Ma, Qiang Kang

Received: 14 April 2013/Revised: 18 June 2013/Accepted: 26 August 2013/Published online: 10 October 2013
© The Nonferrous Metals Society of China and Springer-Verlag Berlin Heidelberg 2013

Abstract To develop a new magnesium alloy with excellent formability at room temperature, the effect of Y, Ce, and Gd addition on texture and stretch formability of Mg–1.5Zn alloys was carried out. The result shows that Y, Ce, and Gd addition in Mg–1.5Zn alloys can effectively weaken and modify the basal plane texture, characterized by TD-split texture in which the position of basal is tilted from normal direction (ND) toward transverse direction (TD). When Mg–1.5Zn alloy with Gd addition appears low texture intensity and TD-split texture, where the position of basal poles is tilted by about $\pm 35^\circ$ from ND toward to TD, the largest Erichsen value of 7.0 and the elongation rate reaches 29.1 % in TD direction. However, Y and Ce addition in Mg–1.5Zn alloys promote a large number of second phase particles, which cancel the contribution of the unique basal texture to stretch formability and ductility.

Keywords Magnesium; Texture; Size effects; Stretch formability; Mechanical property; Rare earth elements

1 Introduction

Improving fuel efficiency and reducing emissions of vehicles can be achieved through lightweight construction. Mg and its alloys, as the lightest construction metals, offer a remarkable potential in this regard [1]. In Mg, the (0002) $\langle 11\text{--}20 \rangle$ basal slip takes place preferentially because the critical resolved shear stress (CRSS) for the

basal slip is lower than those for the non-basal slips, that is, the prismatic and pyramidal slips [2]. Five independent slip systems are necessary to make a polycrystalline material undergo a general homogeneous deformation without producing cracks. However, the basal slip has only two independent slip systems [3]. This gives rise to poor ductility and formability for polycrystalline Mg and its alloy, thereby limiting their applications. In addition, for rolled Mg alloy sheets, the (0002) basal plane is strongly distributed parallel to the RD–TD plane, where the RD and TD are the rolling and transverse directions. In such a case, it is very difficult for the textured sheets to be deformed in the thickness direction [4], resulting in a poor stretch formability.

To improve the formability, many processing technologies are introduced into magnesium alloys and proved to be effective in developing weaker or non-basal textures, e.g., equal channel angular extrusion (ECAE) [5], differential speed rolling [6], and torsion extrusion [7]. However, these processing technologies are not as efficient as rolling process. Another way to weak basal texture is therefore necessary. It was recently found that magnesium alloys with rare earth were observed to develop more random texture during conventional hot rolling [8]. Mg addition of 0.2 wt%Ce decreases the (0002) plane texture intensity compared with pure Mg, and leads the (0002) plane texture distributed parallel to RD [9]. The tendency to split basal intensity in the rolling direction may be enhanced by an increase in the activity of pyramidal slips [10]. Another possibility for the splitting of the basal plane is the occurrence of double twinning [8], which is $\{10\text{--}11\}$ twinning followed by $\{10\text{--}12\}$ re-twinning. The same trend was obtained in Mg–Gd alloy. Therefore, it is suggested that not only the basal slip, but also the other deformation mechanisms are active in the Mg–RE alloy.

Z.-X. Cai, H.-T. Jiang*, D. Tang, Z. Ma, Q. Kang
National Engineering Research Center of Advanced Rolling,
University of Science and Technology Beijing, Beijing 100083,
China
e-mail: nwpujht@163.com

Recently, the addition of rare-earth metal to Mg–Zn alloy has been found to be an effective way of weakening and changing the basal texture of wrought magnesium alloys [11–15], and the Mg alloy exhibits an excellent workability [16]. But the effect of RE type on weakening the texture and improving the ductility and formability of Mg were not studied systematically. However, adding too much of these elements causes poor ductility [17] because of an excessive solid-solution strengthening mechanism. Moreover, too little addition induces no solid-solution effects [18]. Hence, in this paper, the 0.2 wt%RE (Gd, Ce, Y) as major alloying element was added in Mg–1.5Zn alloy separately and the texture ductility, and stretch formability were studied. In order to take a comparison test, the Mg–1.5Zn was prepared.

2 Experimental

Four magnesium alloys denoted as Mg–1.5Zn, Mg–1.5Zn–0.2Y, Mg–1.5Zn–0.2Ce, and Mg–1.5Zn–0.2Gd were examined in this study. The chemical compositions of the four alloys are listed in Table 1. The alloys were prepared with high purity Mg(99.9 %), Zn(99.9 %), and Mg–30 %RE by vacuum melting. Ingots were prepared by pouring the melt into a preheated steel mold. The ingots were homogenized at 450 °C for 12 h and then quenched in water. The ingots were subsequently machined to slabs with a dimension of 120 mm × 90 mm × 10 mm. The slabs were rolled to sheets with a final thickness of 1 mm at a reduction of 15 %–20 % per pass. After each pass, the sheets were reheated to 450 °C and held for 15 min to maintain a consistent rolling temperature. Then the sheets were annealed at 350 °C for 1 h.

For optical microscopy (OM), specimens were etched for 20 s in acetic picral (10 ml water + 5 g picric acid + 5 ml acetic acid + 100 ml ethanol). The precipitates image and fractograph were examined by scanning electron microscopy (SEM, ZEISS ULTRA 55) with energy dispersive spectroscopy (EDS). The (0002) plane pole figure of the rolled Mg alloys at surface was investigated by Schulz reflection method, texture measurements by means of X-ray diffraction (XRD) were performed on Siemens D5000. Tensile specimens with a 6 mm gauge

width and a 25-mm gauge length were machined from the sheets in three orientations: rolling direction (RD), 45° to RD, and transverse direction (TD). Tensile tests were carried out at room temperature with an initial strain rate of $1 \times 10^{-3} \text{ s}^{-1}$ on a universal testing machine.

A circular blank with a diameter of 60 mm was machined from the rolled and subsequently annealed specimens. Erichsen tests using a hemispherical punch with a diameter of 20 mm were carried out at room temperature to investigate the stretch formability of the specimens, and Erichsen value (*IE*), which was the punch stroke at fracture initiation, was measured. The punch speed and blank holder force were $0.1 \text{ mm}\cdot\text{s}^{-1}$ and 10 kN, respectively. Erichsen tests were measured by Zwick/Roell BPB600.

3 Results and discussion

3.1 Microstructure and texture

The microstructures of the rolled and subsequently annealed Mg–1.5Zn and Mg–1.5Zn–0.2RE alloys in the RD–TD plane are shown in Fig. 1. The result shows that all alloys are recrystallized completely, the average grain sizes of the alloys are 52 μm for the Mg–1.5Zn, 15 μm for the Mg–1.5Zn–0.2Y, 17 μm for the Mg–1.5Zn–0.2Ce, 25 μm for the Mg–1.5Zn–0.2Gd alloys. The microstructures of four alloys are quite different, although the four alloys undergo the same rolled and annealed condition. So the effect on microstructure of Mg alloy is not only on the content, but also obviously on the type of RE addition in Mg. Figure 2 is the SEM images of the four alloys. In the SEM images, the microstructures contain varying amount of precipitates with different compositions. EDS analysis of the four alloys shows that precipitates consist of Zn, RE, and Mg (Table 2). There are very few precipitates in Mg–1.5Zn. All the RE-containing alloys have precipitates containing Mg, Zn, and RE elements, and the amount of precipitates of Mg–1.5Zn–0.2Y and Mg–1.5Zn–0.2Ce alloys are more than Mg–1.5Zn–0.2Gd alloy, leading to the grain size of the two alloys smaller than Mg–1.5Zn–0.2Gd alloy (Fig. 1).

Figure 3 shows the (0002) and (10–10) pole figures of rolled and subsequently annealed Mg–1.5Zn and Mg–

Table 1 Chemical compositions of alloys (wt%)

Alloys	Zn	RE	Fe	Cu	Ni	Mg
Mg–1.5Zn	1.48	0	0.0042	0.0023	<0.0001	Bal.
Mg–1.5Zn–0.2Y	1.44	0.18	0.0035	0.0020	<0.0001	Bal.
Mg–1.5Zn–0.2Ce	1.45	0.18	0.0031	0.0021	<0.0001	Bal.
Mg–1.5Zn–0.2Gd	1.46	0.17	0.0032	0.0020	<0.0001	Bal.

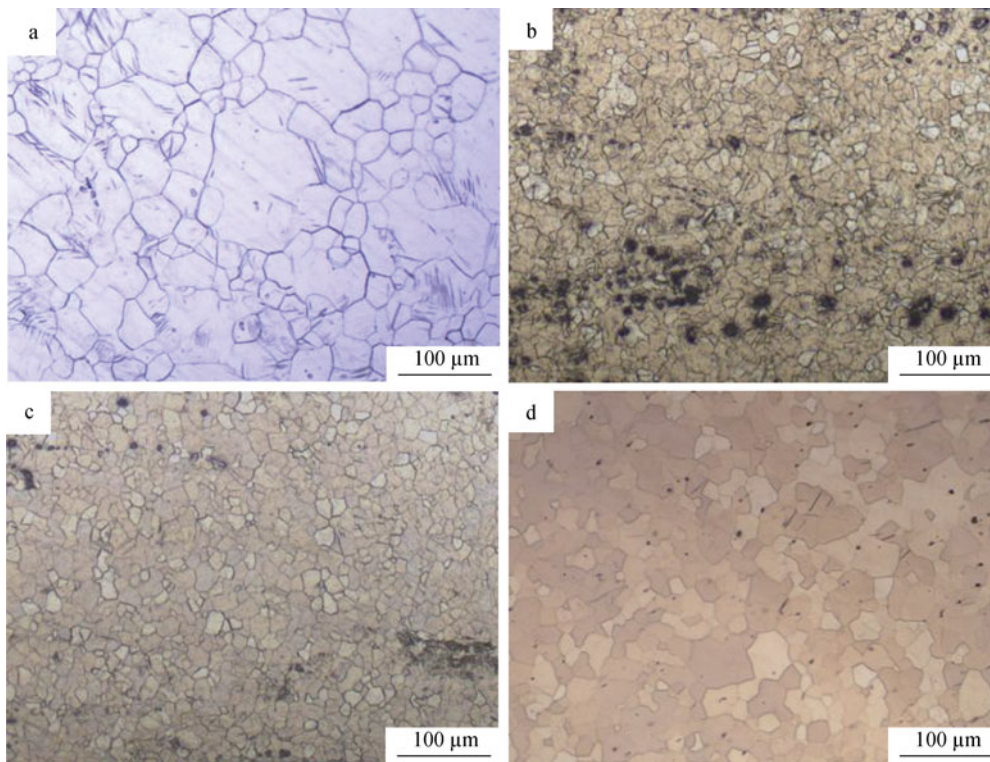


Fig. 1 OM images of rolled and subsequently annealed Mg alloys: **a** Mg–1.5Zn, **b** Mg–1.5Zn–0.2Y, **c** Mg–1.5Zn–0.2Ce, and **d** Mg–1.5Zn–0.2Gd

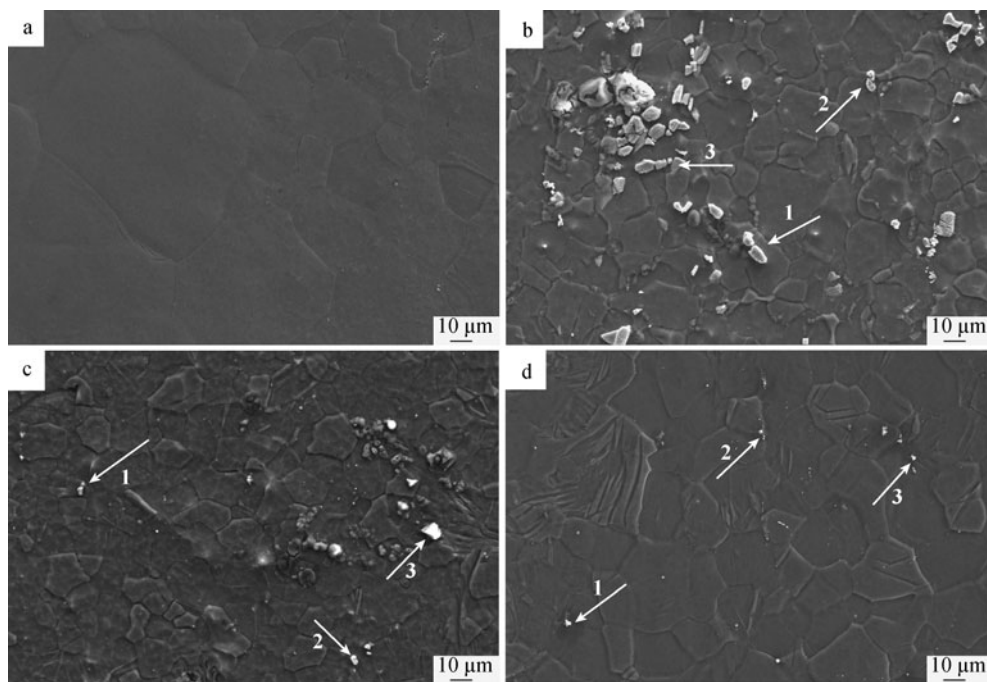


Fig. 2 SEM images showing precipitates of Mg alloys: **a** Mg–1.5Zn, **b** Mg–1.5Zn–0.2Y, **c** Mg–1.5Zn–0.2Ce, and **d** Mg–1.5Zn–0.2Gd

1.5Zn–0.2RE alloys. It can be found that the addition of RE effectively weakens the basal texture intensity, and exhibits low basal texture intensity, whose value is much lower than

that of AZ31 alloy sheets (from 6 to 8) [18]. It is known that the basal plane of AZ31 alloy sheet is intensively distributed parallel to the RD-TD plane, and there is a

Table 2 EDS analysis of particles as shown in SEM images in Fig. 2 (wt%)

Alloys	Particle	Mg	Zn	RE
Mg–1.5Zn–0.2Y	1	55.7	16.6	27.7
	2	65.4	10.5	24.1
	3	67.7	22.5	9.8
Mg–1.5Zn–0.2Ce	1	77.5	18.2	4.3
	2	85.8	11.4	2.8
	3	67.9	13.7	8.4
Mg–1.5Zn–0.2Gd	1	51.3	21.1	28.6
	2	75.9	16.6	7.5
	3	51.3	30.5	18.2

spreading of the basal poles toward RD [19]. On the other hand, the peak intensity of the Mg–1.5Zn–0.2RE alloys exhibits the TD split texture, where the position of basal poles is tilted by about $\pm 25^\circ$, $\pm 27^\circ$, and $\pm 35^\circ$ from ND to TD for Mg–1.5Zn–0.2Y, Mg–1.5Zn–0.2Ce, and Mg–1.5Zn–0.2Gd alloys. Moreover, it should be noted that the clear splitting of basal poles toward TD observed in the annealed specimen is not observed in the Mg–1.5Zn alloy, during the same rolled and subsequently annealed condition. Evidently, RE elements change the deformation and recrystallization mechanism of Mg (deformation and recrystallization behavior strongly affects texture formation).

All the RE-containing Mg alloys examined in this study have lower basal pole intensity parallel to ND, and the highest intensity point is tilted away from the ND to TD,

but the texture distribution and texture strength have some differences (as shown in Fig. 3) which maybe caused by the type of rare-earth adding in Mg alloys.

3.2 Stretch formability and mechanical properties at room temperature

The Erichsen tests of the rolled and subsequently annealed Mg–1.5Zn and Mg–1.5Zn–0.2RE alloys are summarized in Fig. 4. The result shows that the *IE* value of the alloys are 2.6 for the Mg–1.5Zn, 4.9 for the Mg–1.5Zn–0.2Y, 5.8 for the Mg–1.5Zn–0.2Ce, 7.0 for the Mg–1.5Zn–0.2Gd. The Mg–1.5Zn–0.2Gd alloy exhibits significant stretch formability (*IE* = 7.0), which is approach to that of 5000 and 6000 series Al alloy and the stretch formability of Mg–1.5Zn–0.2Ce and Mg–1.5Zn–0.2Y decrease gradually. It is shown that the type of RE addition in Mg alloy can affect the stretch formability of Mg alloy at room temperature.

The tensile properties of the rolled and subsequently annealed Mg–1.5Zn and Mg–1.5Zn–0.2RE alloys are summarized in Table 3. Mg–1.5Zn alloy exhibits a yield anisotropy typical of conventional magnesium alloys, such as AZ31B. The highest yield strength is measured along the TD and the lowest along the RD. Additionally, the yield point is much more pronounced in the TD than in any other orientation. The elongation-to-failure is slightly higher in RD than in other orientations. The tensile strength and strain-hardening behavior are rather low and similar along the different directions.

In comparison with this behavior of Mg–1.5Zn alloy sheets, the results obtained from the RE-containing alloys

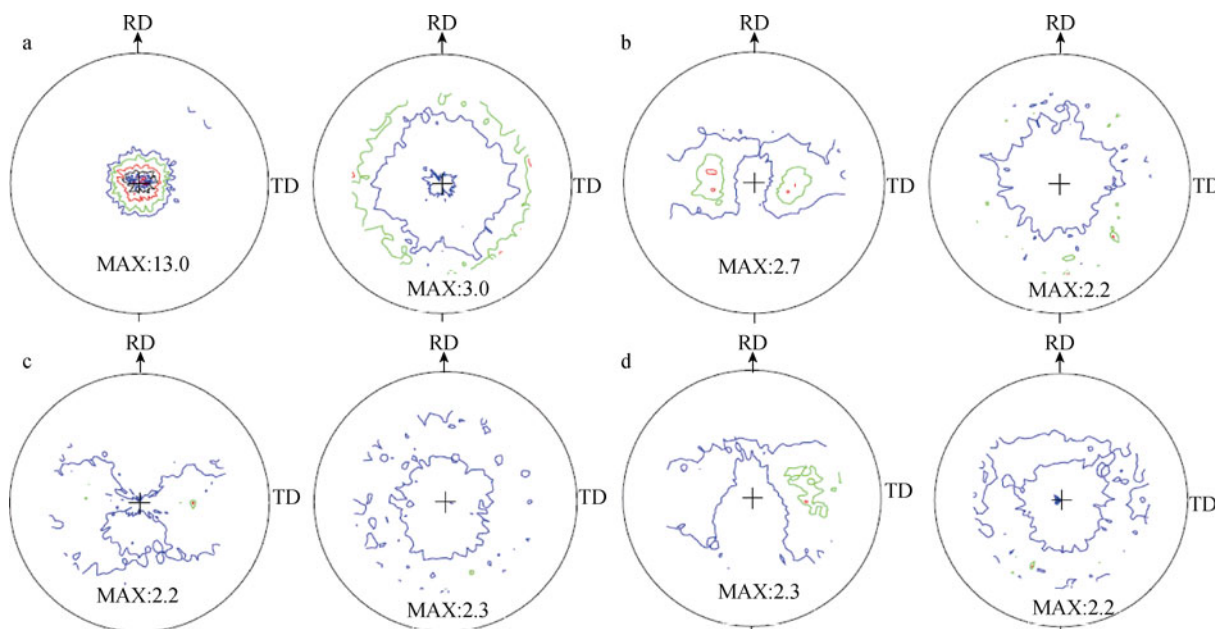


Fig. 3 (0002) and (10–10) plane pole figures of rolled and subsequently annealed Mg alloys: **a** Mg–1.5Zn, **b** Mg–1.5Zn–0.2Y, **c** Mg–1.5Zn–0.2Ce, and **d** Mg–1.5Zn–0.2Gd

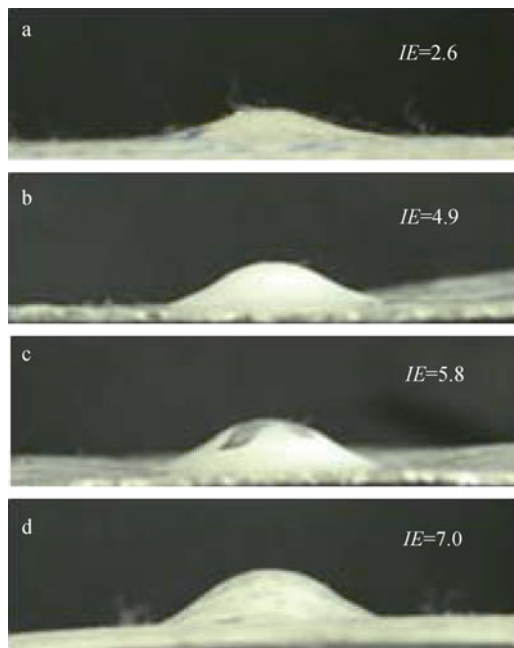


Fig. 4 Erichsen test of Mg alloys at room temperature: **a** Mg–1.5Zn, **b** Mg–1.5Zn–0.2Y, **c** Mg–1.5Zn–0.2Ce, and **d** Mg–1.5Zn–0.2Gd

are in many ways opposite. The yield and tensile strength are the highest in the RD and decreases toward the TD. The elongation-to-failure is the lowest along the RD. And it is worthy of special mentioning that the tensile properties of Mg–1.5Zn–0.2Y and Mg–1.5Zn–0.2Ce alloys exhibit lower elongation, higher strength, and higher yield stress compared with those of Mg–1.5Zn–0.2Gd alloy at all directions. The strengthening behavior of the Mg–1.5Zn–0.2Y and Mg–1.5Zn–0.2Ce alloys is likely attributed to the presence of large MgZnRE phase particles.

It is known that the press formability of sheets at room temperature is strongly affected by the Lankford value (r -value). The average r -values of all Mg–1.5Zn–0.2RE

specimens ($r_{\text{ave}} \leq 0.77$) are much lower than that of conventional Mg alloys ($r_{\text{ave}} = 3.1$) [4]. The low r -value indicates that sheet thinning can easily occur during in-plane tensile deformation. And all the r -values of Mg–1.5Zn–0.2RE specimens at TD are the lowest, this trend in the r -value can be explained by the distribution and intensity of the TD-split texture.

Figure 5 shows the fracture surface after tensile test of the rolled and subsequently annealed Mg–1.5Zn and Mg–1.5Zn–0.2RE alloys, where the angle between tensile direction and RD is 0° (in order to describe the organization of the fracture morphology, Mg–1.5Zn and Mg–1.5Zn–0.2RE alloys have different magnifications). In Mg–1.5Zn alloy, the fracture surfaces are composed of cleavage planes (as shown in Fig. 5a), which is in accordance with its limited elongation of 16.4 %. The fracture model of Mg–1.5Zn alloy is cleavage. When the Mg–1.5Zn alloy is added with 0.2 wt%RE(Gd, Ce, Y), the fracture surfaces are much different from Mg–1.5Zn alloy, and it exhibit mixed characteristics of brittleness and ductility (as shown in Fig. 5b–d), which is in accordance with its high elongation (greater than 20 %). The fracture model of Mg–1.5Zn–0.2RE alloys are quasi-cleavage.

While the fractograph of the three Mg–1.5Zn–0.2RE alloys has some difference. The fracture surface of Mg–1.5Zn–0.2Gd alloy have large numbers of dimples and a few tear ridges, and it experiences sufficient plastic deformation before fracture failure, so it has better ductility than the others. In addition, the second phase particles of Mg–1.5Zn–0.2Gd alloy are much less and smaller on the fracture surface than the others. In general, hard second phase particles in a metallic material often become the sites for stress concentration and void nucleation. Therefore, much more second phase particles may cancel the contribution of the unique basal texture to stretch formability and ductility. Mg–1.5Zn alloy addition of 0.2 wt%Y and 0.2 wt%Ce may

Table 3 Tensile properties of rolled and subsequently annealed Mg–1.5Zn and Mg–1.5Zn–0.2RE alloys at room temperature

Alloys	Direction	Yield stress/MPa	Tensile stress/MPa	Elongation/%	n	r	r_{ave}
Mg–1.5Zn	RD	106.6	195.2	16.4	0.25		
	45°	108.9	193.4	14	0.24		
	TD	113.4	187.8	9.3	0.26		
Mg–1.5Zn–0.2Y	RD	138.7	236.2	18.9	0.25	0.61	0.75
	45°	125.7	228.0	26.7	0.26	0.92	
	TD	106.1	222.0	21.3	0.24	0.56	
Mg–1.5Zn–0.2Ce	RD	142.3	236.1	20.3	0.27	0.75	0.77
	45°	126.4	224.3	21.7	0.27	0.81	
	TD	92.3	217.1	22.4	0.26	0.71	
Mg–1.5Zn–0.2Gd	RD	126.5	216.6	26.7	0.27	0.78	0.75
	45°	90.4	205.5	28.9	0.33	0.82	
	TD	69.7	202.3	29.1	0.45	0.57	

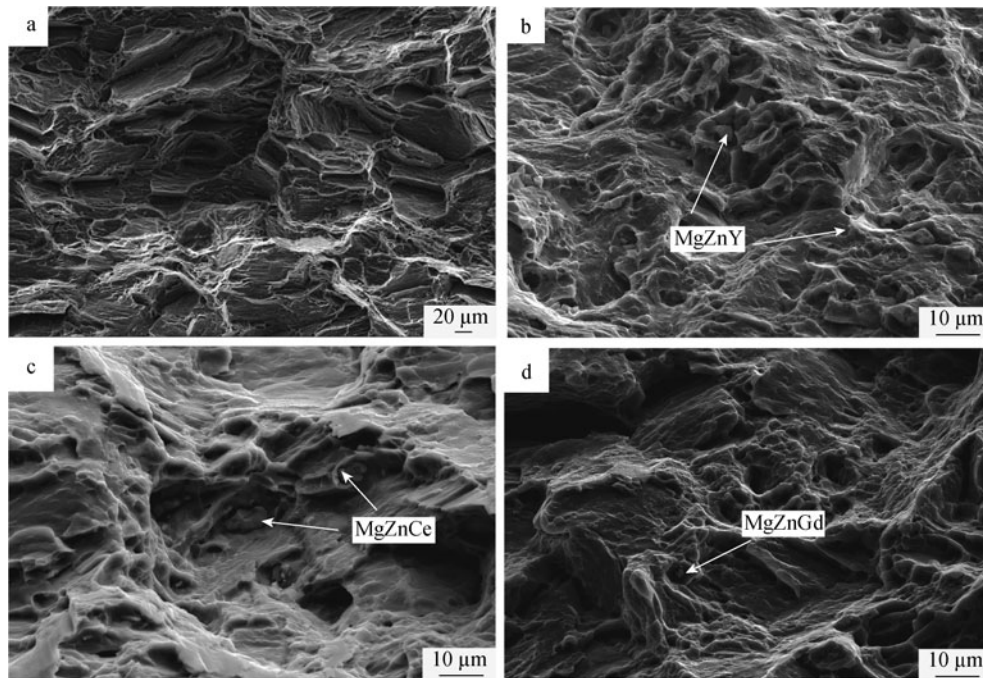


Fig. 5 SEM images after tensile test of the rolled and subsequently annealed Mg alloys: **a** Mg–1.5Zn, **b** Mg–1.5Zn–0.2Y, **c** Mg–1.5Zn–0.2Ce, and **d** Mg–1.5Zn–0.2Gd

produce much more second phase particles than 0.2 wt%Gd (as shown in Figs. 1, 2, and 5), so it is another reason that Mg–1.5Zn–0.2Gd alloy has better ductility than Mg–1.5Zn–0.2Y alloy and Mg–1.5Zn–0.2Ce alloy.

4 Conclusion

The texture and stretch formability of Mg–1.5Zn alloys containing Y, Ce, and Gd at room temperature were investigated. It is demonstrated that dilute Y, Ce, and Gd addition in Mg–1.5Zn alloy effectively weakens and modifies the basal texture, characterized by the splitting basal pole toward TD. The unique basal texture contributes to the significant improvement of stretch formability. However, Y and Ce addition in Mg–1.5Zn alloys promote a large number of second phase particles, resulting in the deterioration of stretch formability.

Acknowledgments This study was financially supported by the Ministry of Science and Technology “Twelfth Five-Year” Plan for Science & Technology Support (No. 2011BAE22B00).

References

[1] Friedrich H, Schumann S. Research for a “new age of magnesium” in the automotive industry. *J Mater Process Technol.* 2001;117(3):276.

- [2] Yoshinaga H, Horiuchi R. Deformation mechanisms in magnesium single crystals compressed in the direction parallel to hexagonal axis. *Trans JIM.* 1963;4:1.
- [3] Yoo MH. Slip, twinning, and fracture in hexagonal close-packed metals. *Metall Trans A.* 1981;12(3):409.
- [4] Chino Y, Iwasaki H, Mabuchi M. Stretch formability of AZ31Mg alloy sheets at different testing temperatures. *Mater Sci Eng A.* 2007;466(1–2):90.
- [5] Mukai T, Yamanoi M, Watanabe H, Higashi K. Ductility enhancement in AZ31 magnesium alloy by controlling its grain structure. *Scr Mater.* 2001;45(1):89.
- [6] Watanabe H, Mukai T, Ishikawa K. Effect of temperature of differential speed rolling on room temperature mechanical properties and texture in an AZ31 magnesium alloy. *J Mater Process Technol.* 2007;182(1–3):644.
- [7] Chino Y, Sassa K, Mabuchi M. Enhancement of tensile ductility of magnesium alloy produced by torsion extrusion. *Scr Mater.* 2008;59(4):399.
- [8] Bohlen J, Nurnberg MR, Senn JW, Letzig D, Agnew SR. The texture and anisotropy of magnesium–zinc–rare earth alloy sheets. *Acta Mater.* 2007;55(6):2101.
- [9] Chino Y, Kado M, Mabuchi M. Compressive deformation behavior at room temperature–773K in Mg–0.2 mass% (0.035at%)Ce alloy. *Mater Sci Eng.* 2008;494(3):343.
- [10] Agnew SR, Yoo MH, Tome CN. Application of texture simulation to understanding mechanical behavior of Mg and solid solution alloys containing Li or Y. *Acta Mater.* 2001;49(20):4277.
- [11] Wu D, Chen RS, Tang WN, Han EH. Influence of texture and grain size on the room-temperature ductility and tensile behavior in a Mg–Zn–Gd alloy processed by rolling and forging. *Material and Design.* 2012;41:306.
- [12] Wu D, Chen RS, Han EH. Excellent room-temperature ductility and formability of rolled Mg–Zn–Gd alloy sheets. *J Alloy Compd.* 2011;509(6):2856.

- [13] Yan H, Chen RS, Han EH. Room-temperature ductility and anisotropy of two rolled Mg–Zn–Gd alloys. *Mater Sci Eng.* 2010;527(15):3317.
- [14] Chino Y, Sassa K, Mabuchi M. Texture and stretch formability of a rolled Mg–Zn alloy containing dilute content of Y. *Mater Sci Eng A.* 2009;513–514:394.
- [15] Chino Y, Huang XS, Suzuki K, Sassa K, Mabuchi M. Influence of Zn concentration on stretch formability at room temperature of Mg–Zn–Ce alloy. *Mater Sci Eng A.* 2010;528(2):566.
- [16] Chen Q, Lin J, Shu DY, Hu CK, Zhao ZD, Kang F, Huang SH, Yuan BG. Microstructure development, mechanical properties and formability of Mg–Zn–Y–Zr magnesium alloy. *Mater Sci Eng A.* 2012;554:129.
- [17] McDonald JC. Tensile properties of rolled magnesium alloys—binary alloys with calcium, cerium, gallium, and thorium. *Trans AIME.* 1941;138:179.
- [18] Akhtar A, Teghtsoonian E. Solid solution strengthening of magnesium single crystals—ii the effect of solute on the ease of prismatic slip. *Acta Metall.* 1969;17(11):1339.
- [19] Jeong HT, Ha TK. Texture development in a warm rolled AZ31 magnesium alloy. *J Mater Process Technol.* 2007;187–188:559.